Biochemical and Biophysical Research Communications 452 (2014) 415–421

Contents lists available at ScienceDirect

Biochemical and Biophysical Research Communications

journal homepage: www.elsevier.com/locate/ybbrc

Urinary *Xist* is a potential biomarker for membranous nephropathy

Yen-Sung Huang [a], Hsin-Yi Hsieh [b], Hsiu-Ming Shih [a], Huey-Kang Sytwu [c], Chia-Chao Wu [b,c,*]

[a] Institute of Biomedical Sciences, Academia Sinica, Taiwan
[b] Division of Nephrology, Department of Internal Medicine, Tri-Service General Hospital, National Defense Medical Center, Taiwan
[c] Department and Graduate Institute of Microbiology and Immunology, National Defense Medical Center, Taiwan

ARTICLE INFO

Article history:
Received 9 August 2014
Available online 23 August 2014

Keywords:
LncRNA
Xist
Membranous nephropathy
H3K27me3

ABSTRACT

Membranous nephropathy (MN), a type of glomerular nephritis, is the most common cause of nephrotic syndrome in human adults. Changes in gene expression as a result of epigenetic dysregulation through long noncoding RNAs (lncRNAs) are increasingly being recognized as important factors in disease. Using an experimental MN mouse model, we identify the first dysregulated lncRNAs, *Xist* and *NEAT1*, whose levels are significantly upregulated in both tubular epithelial and glomerular cells. MN is also often characterized by glomerular podocyte injury. Treatment of a mouse podocyte cell line with lipopolysaccharides to induce injury resulted in the stable elevation of *Xist*, but not *NEAT1* levels. In mice, the observed changes in *Xist* levels are specific: *Xist* can be effectively detected in urine, with a strong correlation to disease severity, but not serum in MN samples. We find that regulation of *Xist* may be controlled by post-translational modifications. H3K27me3 levels are significantly downregulated in mouse MN kidney, where chromatin immunoprecipitation experiments also showed decreased H3K27me3 at *Xist* promoter regions. Finally, we show that our findings in mice can be extended to human clinical samples. Urinary *Xist* is significantly elevated in urine samples from patients with different types of glomerular nephritis, including MN, compared to normal counterparts. Together, our results suggest that a reduction of H3K27me3 at *Xist* promoter regions leads to elevated levels of urinary *Xist*, which may be used as a biomarker to detect MN.

1. Introduction

Membranous nephropathy (MN), an autoimmune-mediated glomerular nephritis characterized by *in situ* immune complex deposition in the subepithelial space, is the most prevalent cause of nephrotic syndrome in human adults [1,2]. In most MN cases, deposition of immune complexes and subsequent responses, such as inflammatory cytokines, complement activation, and oxidative stress, are all involved in its pathogenesis [3,4]. Approximately 30–40% of patients with MN develop progressive renal impairment, which results in end-stage renal failure after 10–15 years [5]. Treatment for MN remains controversial and challenging due to persistent adverse effects and a lack of specificity in present immunosuppressive therapy [6]. Thus, there is a need for identification of the regulatory mechanisms involved, and development of biomarkers for early diagnosis and discrimination of MN severity.

A large part (up to 70%) of the human genome is transcribed, while only 2% encodes for proteins [7]. Recent studies have shown that a subtype of noncoding RNAs, long noncoding RNAs (lncRNAs), play important roles in disease [8]. A major function of lncRNAs is modulation of the epigenetic status of protein-coding genes through cis- and trans-acting mechanisms, such as recruitment of chromatin remodeling complexes to specific genomic loci [9]. Importantly, lncRNAs are often expressed in a disease-, tissue-, or developmental stage-specific manner, which makes these molecules attractive candidates for biomarkers and therapeutic targets [10]. However, current knowledge of lncRNA function remains limited to cancers, and some cardiovascular and neurodegenerative diseases [11]. This study identifies the first dysregulated lncRNAs in an experimental MN model.

2. Materials and methods

2.1. Animal

All animal procedures were performed according to IACUC-approved protocol (TSGH 12-280). 6 week-old female BALB/C (National Laboratory Animal Center, Taiwan) mice were maintained

* Corresponding author at: Division of Nephrology, Department of Internal Medicine, Tri-Service General Hospital, National Defense Medical Center, 325 Cheng-Kung Road, Section 2, Nei-Hu, Taipei 11490, Taiwan.
E-mail address: wucc@mail.ndmctsgh.edu.tw (C.-C. Wu).

http://dx.doi.org/10.1016/j.bbrc.2014.08.077
0006-291X/

in micro-isolators in pathogen-free conditions. At the end of experiments, mice were sacrificed for kidney and spleen removal.

2.2. Murine model of membranous nephropathy

Membranous nephropathy was induced as previously described [12,13]. Both control and experimental groups were immunized with 0.2 mg cationic bovine serum albumin (cBSA; Chondrex, Redmond, USA) emulsified in an equal volume of complete Freund's adjuvant (Sigma, St. Louis, USA). After 2 weeks, mice from the experimental group were injected intravenously with 5 (low-lose) or 13 (high-dose) mg/kg of cBSA 3 times weekly for an additional 6 weeks. Mice from the control group received saline according to the same schedule.

2.3. Quantitative RT-PCR (RT-qPCR)

See Supplementary content for details.

2.4. Hematoxylin and eosin staining (HE), immunofluorescence (IF) and immunohistochemistry (IHC)

Renal tissue samples were prepared by snap-freezing, then fixed with acetone for IF or 10% formalin for HE and IHC. HE staining, IF and IHC were performed as previously described [14,15]. Frozen sections were incubated with fluorescein isothiocyanate-conjugated goat anti-mouse IgG and C3 (Capple, Durham, USA). Paraffin embedded sections were incubated with antibodies listed in Table S2, stained with the Vectastain Elite ABC kit (Vector Lab, Burlingame, CA), developed using DAB (brown precipitate, Vector Lab), and observed using a fluorescence and light microscope (Olympus, Tokyo, Japan).

2.5. RNA in situ hybridization (ISH) on frozen tissues

ISH was performed according to QuantiGene ViewRNA protocols. 5 μm sections were cut, boiled in pre-treatment solution, and digested with proteinase K. Sections were hybridized with custom-designed QuantiGene ViewRNA probes against *NEAT1* and *Xist*. Bound probes were then amplified using PreAmp and Amp molecules (all reagents from Affymetrix, Santa Clara, USA). Multiple Label Probe oligonucleotides conjugated to alkaline phosphatase were then added and Fast Red Substrate used to produce signal (Cy3). Images were collected on a spinning disk confocal microscope (Ultra View; PerkinElmer, Boston, USA). Fluorescence intensity was measured using MetaMorph software.

2.6. Protein extraction and western blot analysis

See Supplementary content for details.

2.7. Chromatin immunoprecipitation quantitative PCR (ChIP-qPCR) assay

ChIP was performed as previously described [16]. ChIP product was analyzed by quantitative real-time PCR using the Applied Biosystem 7500 Real-Time PCR System. Experiments were done in triplicate. A fraction (1%) of the sonicated chromatin was set aside as input control before antibody affinity manipulations. Percent input was calculated by $100 \times 2\text{^}(Ct^{\text{adjusted Input}} - Ct^{IP})$. Purified DNA was subjected to qPCR, using specific primers for mouse *Xist* promoter: region 1 (−399 to −473), 5′-TGAGCGTAAGCCCACC AAAT-3′ and 5′-TGCCTCACAAAATGGCTCCT-3′; region 2 (−4 to −70), 5′-GCAATCTTTGTGGCCACTCC-3′ and 5′-CACGCCTTTA ACTG ATCCGC-3′.

2.8. Cell culture and treatment of cultured podocytes with lipopolysaccharide (LPS)

E11 podocytes were obtained from the CLS cell lines service. The E11 cell lines, previously described in detail [17], were maintained in RPMI-1640 supplemented with 10% fetal bovine serum (FBS), and penicillin/streptomycin at 33 °C under a humidified atmosphere of 5% CO^2. E11 cells at 50% confluence were thermo-switched from 33 °C to 38 °C for 14 days. Differentiated podocytes were maintained in serum-free RMPI-1640 for 24 h prior to treatment with purified *Escherichia coli* LPS from the O111:B4 strain (Sigma). Experiments were conducted in triplicate using 50 ug/ml LPS to study RNA expression by RT-qPCR at 1 h and 6 h.

2.9. Collection of urine samples and RNA isolation

A total 20 urine samples from 8 normal and 12 patients diagnosed with glomerular nephritis (at the Division of Nephrology, Tri-Service General Hospital, Taiwan) were obtained. All Institutional Review Board-approved protocols (TSGH 102-05-020) were followed. Total RNA was extracted from urine using TRIzol (Life Technologies). 500 uL urine was mixed with 500 uL TRIzol and 200 uL chloroform, then total RNA was isolated from the resulting supernatant using NucleoSpin RNA II kit (Macherey Nagel). Relative expression was determined by the following calculation where the threshold cycle (Ct) scores of target is normalized to reference (only assays with Ct values below reference = 38.4439) and relative to calibrator sample. Relative expression = $2^{(-\Delta\Delta Ct)}$, where $\Delta\Delta Ct = (Ct_{\text{target}} - Ct_{\text{reference}}) - (Ct_{\text{calibrator sample}} - Ct_{\text{reference}})$.

2.10. Statistical analysis

All analyses performed with SigmaPlot software.

3. Results

3.1. NEAT1 and Xist are upregulated in kidneys with experimental membranous nephropathy

Polycomb repressive complex (PRC2), a key epigenetic regulator in multicellular organisms, catalyzes di- and tri-methylation of lysine 27 on histone H3 (H3K27me2/me3). In mammals, PRC2 plays crucial roles during development and disease pathogenesis. Remarkably, more than 20% of lncRNAs in both human and mouse are bound by PRC2 [18]. Here, lncRNAs can modulate binding between PRC2 subunits, binding affinities of PRC2 for chromatin, and PRC2 catalytic rates [18]. Thus, some of PRC2-binding lncRNAs may be used as biomarkers and therapeutic targets for human disease. To test whether PRC2-binding lncRNAs are dysregulated in kidneys during the pathogenesis of experimental MN, we analyzed publicly-available PRC2 RIP-Seq data sets generated with mouse embryonic stem cells (ESCs) [19]. RPKM (reads per kilobase per million mapped reads) values were compared to select PRC2-binding lncRNAs from the data set. With a stringent threshold of RPKM > 2 to eliminate false positives and background, a total of seventeen lncRNAs were chosen for subsequent testing.

Using a previously described method that induces MN, we immunized mice with either a high or low dose cationic bovine serum albumin (cBSA) to induce two different degrees of kidney damage [12,14]. As shown in Fig. 1A, MN severity correlates with pathological changes in kidney samples, including a diffuse thickening of the glomerular basement membrane, as well as increased levels of complement C3, IgG, and urinary protein (Fig. 1B) when compared to control samples. In these experimental conditions and using quantitative RT-PCR (RT-qPCR), we tested for changes

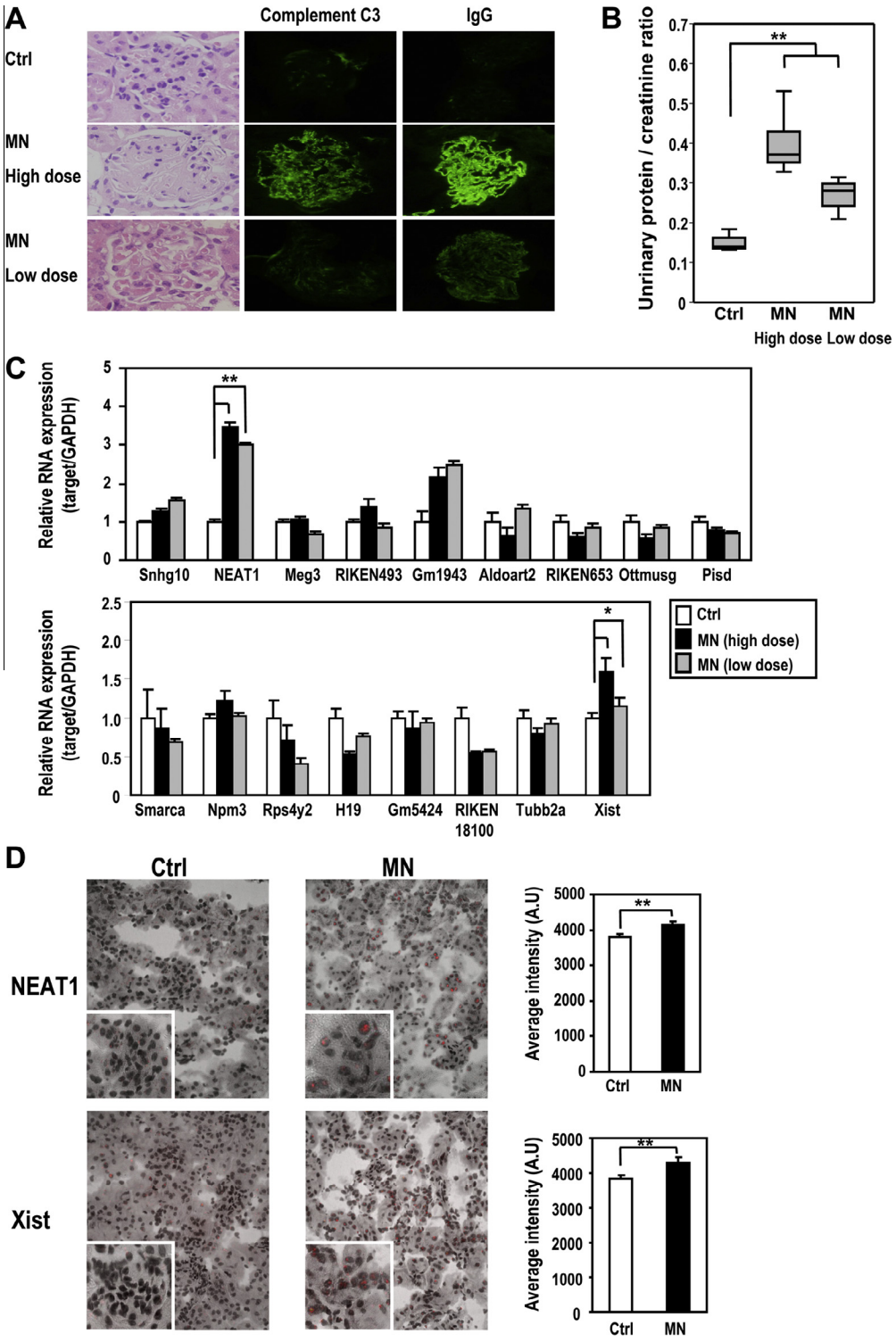

Fig. 1. *NEAT1* and *Xist* are upregulated in kidneys with experimental membranous nephropathy (MN). (A) Kidneys from the control (ctrl) group and MN groups treated with either a high or lose dose of cationic bovine serum albumin (cBSA). Shown are H&E staining (left), and immunofluorescence of complement C3 (middle) and IgG (right). (B) Protein levels in urine expressed as a urinary protein/creatinine ratio. $n = 10$ or 14 mice per group. $^{**}P < 0.01$ (C) RT-qPCR to determine expression level of PRC2-binding lncRNAs from renal tissue of experimental MN or control mice. Data are presented as the mean ± SEM from three mice. $^{*}P < 0.05$; $^{**}P < 0.01$. (D) RNA *in situ* hybridization to visualize *NEAT1* and *Xist* (red) in MN or control kidney samples. Metamorph was used to quantify RNA intensity (right panel), which are shown with arbitrary units (a.u.). (For interpretation of the references to color in this figure legend, the reader is referred to the web version of this article.)

in expression level of PRC2-binding lncRNAs in kidneys. We found *NEAT1* and *Xist* to be significantly elevated in MN kidney samples, with a positive correlation to MN severity (Fig. 1C). Similar results were also observed from glomerulus with MN (data not shown). In addition, we tested two known regulators of *Xist*, *Tsix* (an antisense repressor) and *Jpx* (an activator), that control *Xist* expression by modulating chromatin structure and histone modifications at the *Xist* promoter [20]. RT-qPCR results show that in MN kidneys, *Jpx* is upregulated while *Tsix* becomes downregulated, consistent with an increase in *Xist* expression in affected kidneys (data not shown).

As an independent test for *NEAT1* and *Xist* levels, we used *in situ* hybridization to visualize the lncRNAs; both *NEAT1* and *Xist* levels were increased in tubular epithelial and glomerular cells from MN mice compared to control mice (Fig. 1D).

Podocytes, glomerular epithelial cells, play a critical role in the architecture and function of normal glomerulus. Podocyte injury has been observed in many human and experimental models of glomerular nephritis, including MN, minimal change disease (MCD), rapidly progressive glomerulonephritis (RPGN), and diabetic nephropathy (DN). Lipopolysaccharides (LPS) can induce podocyte injury both *in vitro* and *in vivo* [17], so we treated E11 podocytes with LPS to independently test whether *Xist* and *NEAT1* would become upregulated (Fig. 2A). When treated with LPS, *Xist* expression became stably elevated (both 1 h and 6 h after treatment). *NEAT1* expression, on the other hand, did not maintain its elevated state. Similar to previous results using MN models, we find *Xist* expression to be upregulated in podocyte cells when injury is induced.

3.2. Xist expression is significantly elevated in both ascites and urine of MN mice

In prostate cancer, elevated levels of lncRNAs are released and can be detected in bodily fluids [21]. To test if lncRNAs are similarly released from MN kidneys, we detected *NEAT1*, *Xist*, and *H19* (as a negative control) levels in ascites from experimental MN mice. In line with previous RT-qPCR results, *NEAT1* and *Xist* were highly expressed in ascites, whereas *H19* was not (Fig. S1). Ascites may arise from many different causes, however, and is not specific to kidney failure. Furthermore, not all mice develop ascites, so *NEAT1*, *Xist*, and *H19* expression were also tested in both urine and serum. In urine from MN mice, *Xist* levels were significantly higher than that from control mice, whereas *NEAT1* and *H19* levels were similar between the two groups (Fig. 2B). It is possible that *NEAT1*, essential for the structural integrity and formation of paraspeckles [22], is more retained in the nucleus, and thus not released into urine like *Xist*. Serum from MN and control mice contained similar levels of all tested lncRNAs (Fig. 2C), indicating that the effect is specific to kidney failure. Using urinary protein levels as an indicator for MN severity, we were able to observe a strong positive correlation between urinary *Xist* and MN severity (Fig. 2D).

3.3. H3K27me3 is reduced at Xist promoter regions in MN kidneys

It is well-documented that *Xist* upregulation leads to X chromosome inactivation by recruiting factors that mediate H3K27me3, which represses gene expression across the chromosome [23]. Since we found *Xist* expression to be significantly higher when MN is induced, we wanted to test whether this had any effects on the post-translational modification (PTM) status of MN kidneys. Samples from MN and control groups were compared by Western blot analysis with antibodies against specific modifications (Fig. 3A). Interestingly, elevated *Xist* levels in affected kidneys did not result in more H3K27me3. On the contrary, H3K27me3 levels in MN kidneys were lower than in control kidneys. Alongside H3K27me3, we also compared the methylation patterns at other lysines: H3K9me3 and H3K36me3 were similarly reduced in MN mice, while H3K79me3 was slightly increased (Fig. 3A). Focusing on H3K27me3 (the most reduced modification in MN mice) and H3K79me3 (the only increased modification), immunohistochemistry was employed to independently test differences in PTM status (Fig. 3B). Consistent with Western blot results, we observed decreased H3K27me3 and slightly increased H3K79me3 levels in the glomerular and cortical tubular cells of MN mice compared to control counterparts.

Lower levels of H3K27me3 (an indicator of heterochromatin [24]) and increased H3K79me3 (associated with euchromatin [25]) in MN mice suggests that these modifications control the

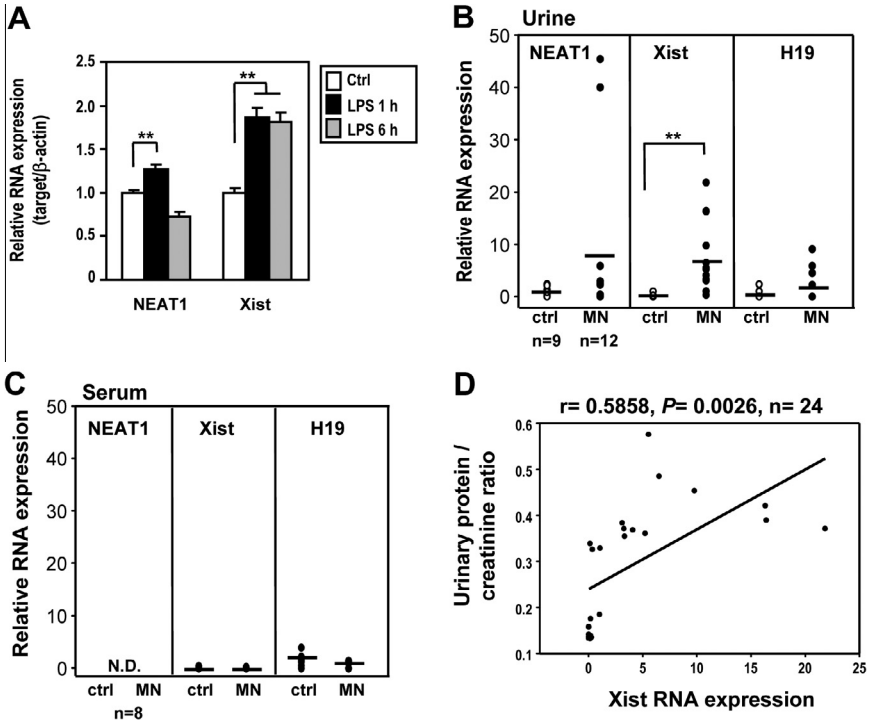

Fig. 2. *Xist* expression is significantly elevated in both LPS-treated podocytes and urine of MN mice. (A) E11 podocyte cells were treated with or without LPS. RNA expression levels from LPS-treated podocytes were determined by RT-qPCR. Data are presented as the mean ± SEM from three independent experiments. $^{**}P < 0.01$. (B and C) RT-qPCR to show relative expression levels of the stated lncRNAs in urine (B) and serum (C) from control (Ctrl) or experimental MN mice. N.D., not detected. $^{**}P < 0.01$. (D) Regression analysis shows a significant correlation between *Xist* expression and urinary protein levels.

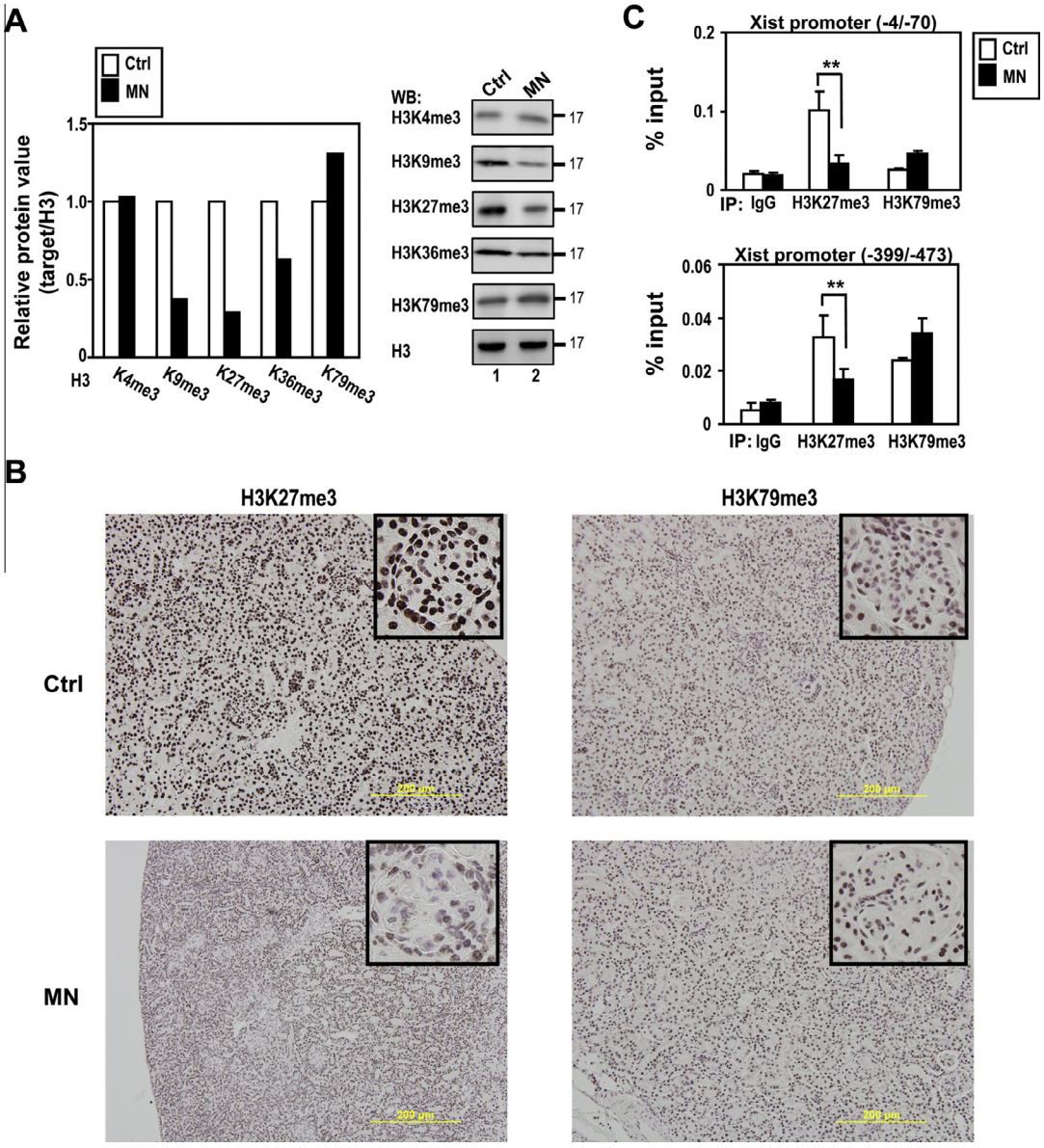

Fig. 3. H3K27me3 is reduced at *Xist* promoter regions in MN kidneys. (A) Lysates from MN renal tissue were immunoblotted with antibodies against the indicated modifications. Relative protein levels were determined by ImageJ densitometry analysis (left panel). (B) Immunohistochemical detection of H3K27me3 and H3K79me3 in renal tissue from MN or control (Ctrl) mice. (C) Chromatin immunoprecipitation (ChIP) assays were performed with antibodies against H3K27me3, H3K79me3, or an IgG control. Subsequent qPCR analysis was carried out using primers specific for 2 promoter regions of *Xist*. Input represents 1% of the chromatin used for immunoprecipitation. Data are presented as the mean ± SEM from three mice. $^{**}P < 0.01$.

expression of *Xist* in disease. To test whether these changes are reflected on the *Xist* promoter, chromatin immunoprecipitation (ChIP) experiments were performed with antibodies against H3K27me3 or H3K79me3 (Fig. 3C). Two distinct promoter regions of *Xist* were tested, and we found significantly decreased H3K27me3 in both regions when comparing MN mice to controls. A slight increase of H3K79me3 at both regions was also observed, although the difference was not statistically significant ($P > 0.05$). Taken together, our data suggests that decreased H3K27me3 at the *Xist* promoter leads to elevated *Xist* expression when MN is induced.

3.4. *Xist* expression is significantly elevated in urine from patients with glomerular nephritis

In both our experimental MN mouse model and LPS-treated podocyte cells, we observed increased *Xist* expression. In the MN mouse model, especially, elevated *Xist* was readily detected in urine, suggesting its potential as a biomarker for MN. To determine if urinary *Xist* is specific for MN in humans, we measured levels of urinary *Xist* and *β-actin* (as a control) from 12 patients with various types of glomerular nephritis, including MN, DN, MCD, RPGN, GN, and 8 normal samples (details are listed in Table S3). Notably, *Xist* expression was significantly increased in patients with glomerular nephritis, including MN, compared to normal counterparts (Fig. 4A); and no differences were apparent in *β-actin* levels between the two groups (Fig. 4B). A positive correlation also exists between urinary *Xist* levels and urinary protein levels ($r = 0.5032$, $P = 0.0237$), but not between urinary *β-actin* levels and urinary protein levels ($r = 0.1622$, $P = 0.4945$). However, we found no correlation between urinary *Xist* levels and specific types of glomerular nephritis (Table S3). Our results suggest that urinary *Xist*, though not specific for MN, can be used as a general biomarker to detect glomerular nephritis.

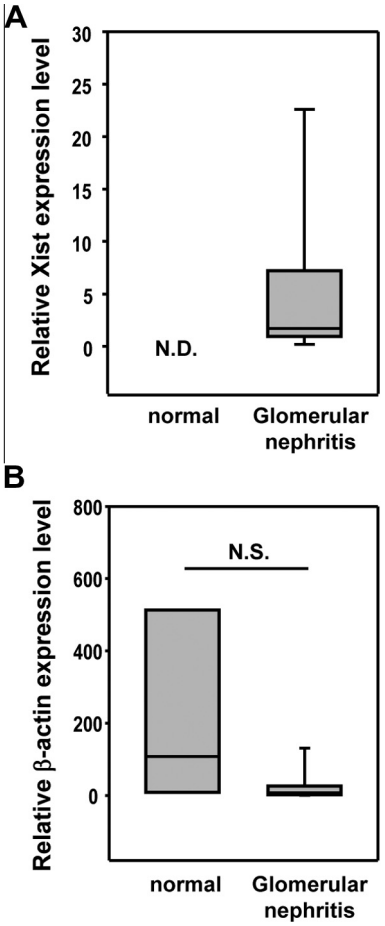

Fig. 4. *Xist* expression is positively correlated with glomerular nephritis incidence in human urine samples. (A and B) RT-qPCR was used to measure RNA expression from normal or glomerular nephritis patient samples. Shown are *Xist* (A) or *β-actin* (B) relative expression levels in normal or glomerular nephritis patient samples. N.D., not detected. N.S., not significant.

4. Discussion

The elevated *Xist* and *NEAT1* expression profiles in experimental MN kidneys highlighted the potential value of these lncRNAs in pathogenic mechanism. *NEAT1* is essential for the structural integrity and formation of paraspeckles [26], which are critical for control of gene expression through the nuclear retention of adenosine-to-inosine editing mRNA [26]. Through this mechanism, paraspeckles and their components may have a role in controlling gene expression during disease processes [26]. Moreover, *Xist* is continuously expressed throughout the female lifespan, decorating the X chromosome during the initiation of X chromosome inactivation [27]. A few recent studies have documented distinct changes in *Xist* expression in response to different stimuli. For example, increased *Xist* levels in the brain were observed when fetal mice were exposed to diesel exhaust [28]. Similar increases in *Xist* expression were also found in response to HDAC inhibitor treatment for breast cancer, or chemotherapy for ovarian cancer [29,30]. These findings raised an interesting question of whether *Xist* can protect cell against damage. However, it remains unclear whether *NEAT1* and *Xist* contribute to MN or if they become altered as a consequence of MN. Further studies are required to dissect the role of *NEAT1* or *Xist* in experimental MN models using conditional gene knockout or transgenic mice studies.

Taken together, our data suggests that decreased H3K27me3 at the *Xist* promoter leads to elevated *Xist* expression when MN is induced. Post-translational modifications of histones often play important roles in the development of diseases [31]. In renal illnesses, for example, it has recently been shown that a global decrease of H3K9me1 indicates poor prognosis for patients with renal cell carcinoma [32]. Here, we find that H3K27me3 is significantly downregulated in kidneys with experimental MN. Further studies, however, are needed to clarify the role of H3K27me3 and its target genes, such as *Xist*, in MN pathogenesis.

The critical 5′ region of *Xist* is well-conserved between human and mouse [33]. Since lncRNAs are more structured and stable than mRNA transcripts, they may be easier to detect in bodily fluids such as urine or blood. Indeed, we find that increased levels of *Xist* can be readily detected in urine collected from both MN mouse model and human glomerular nephritis samples, including MN. Moreover, the function of *Xist* remains largely unknown in males, where it maintains a low expression level. In females, however, *Xist* is important for X chromosome inactivation and is highly expressed [34]. Thus, it may be an especially useful biomarker for females. Accordingly, we find that no significant correlation exists between urinary *Xist* levels and urinary protein levels in male patients with glomerular nephritis, including MN ($r = 0.4767$, $P = 0.0996$, $n = 13$, data not show). Furthermore, proteinuria is one of the most common symptoms of glomerular nephritis. Here, we find a significantly correlation between urinary *Xist* levels and urinary protein levels in experiment MN model and patient with glomerular nephritis. Notably, urinary *Xist* cannot be detected in patient without proteinuria (sample 14 in Table S3). These results further support the notion that urinary *Xist* is a potential biomarker for glomerular nephritis. Clinically, use of urinary *Xist* as a biomarker for glomerular nephritis may help to better identify patients that require hospitalization and urgent immunosuppressive therapy.

Conflict of interest

The authors have declared no conflict of interest.

Acknowledgments

We thank Dr. Shih-Hua Lin and Dr. Jin-Shuen Chen (Division of Nephrology, Department of Internal Medicine, Tri-Service General Hospital, National Defense Medical Center, Taiwan) for their assistance with sample collection. We are grateful to Dr. Teresa Chiang for comments on the paper. This work was supported by grants from the National Science Council (NSC 102-2314-B-016-008-MY3) and the Tri-Service General Hospital (TSGH-C102-009-S04), Taiwan. Part of this work was presented at the annual meeting of the American Society of Nephrology, 5–10 November, 2013, Atlanta, Georgia, as well as at the meeting of The Non-coding Genome, 9–12 October, 2013, EMBL, Heidelberg.

Appendix A. Supplementary data

Supplementary data associated with this article can be found, in the online version, at http://dx.doi.org/10.1016/j.bbrc.2014.08.077.

References

[1] R.J. Glassock, The pathogenesis of idiopathic membranous nephropathy: a 50-year odyssey, Am. J. Kidney Dis. 56 (2010) 157–167.
[2] P. Ronco, H. Debiec, Pathogenesis of membranous nephropathy: recent advances and future challenges, Nat. Rev. Nephrol. 8 (2012) 203–213.
[3] P.N. Cunningham, R.J. Quigg, Contrasting roles of complement activation and its regulation in membranous nephropathy, J. Am. Soc. Nephrol. 16 (2005) 1214–1222.
[4] M. Nangaku, S.J. Shankland, W.G. Couser, Cellular response to injury in membranous nephropathy, J. Am. Soc. Nephrol. 16 (2005) 1195–1204.
[5] D. Cattran, Management of membranous nephropathy: when and what for treatment, J. Am. Soc. Nephrol. 16 (2005) 1188–1194.

[6] R.J. Glassock, The treatment of idiopathic membranous nephropathy: a dilemma or a conundrum?, Am J. Kidney Dis. 44 (2004) 562–566.
[7] M. Guttman, I. Amit, M. Garber, C. French, M.F. Lin, D. Feldser, M. Huarte, O. Zuk, B.W. Carey, J.P. Cassady, M.N. Cabili, R. Jaenisch, T.S. Mikkelsen, T. Jacks, N. Hacohen, B.E. Bernstein, M. Kellis, A. Regev, J.L. Rinn, E.S. Lander, Chromatin signature reveals over a thousand highly conserved large non-coding RNAs in mammals, Nature 458 (2009) 223–227.
[8] A. Troy, N.E. Sharpless, Genetic "lnc"-age of noncoding RNAs to human disease, J. Clin. Invest. 122 (2012) 3837–3840.
[9] P.J. Batista, H.Y. Chang, Long noncoding RNAs: cellular address codes in development and disease, Cell 152 (2013) 1298–1307.
[10] O. Wapinski, H.Y. Chang, Long noncoding RNAs and human disease, Trends Cell Biol. 21 (2011) 354–361.
[11] G. Chen, Z. Wang, D. Wang, C. Qiu, M. Liu, X. Chen, Q. Zhang, G. Yan, Q. Cui, LncRNADisease: a database for long-non-coding RNA-associated diseases, Nucleic Acids Res. 41 (2013) D983–986.
[12] C.C. Wu, K.C. Lu, G.J. Lin, H.Y. Hsieh, P. Chu, S.H. Lin, H.K. Sytwu, Melatonin enhances endogenous heme oxygenase-1 and represses immune responses to ameliorate experimental murine membranous nephropathy, J. Pineal Res. 52 (2012) 460–469.
[13] C.C. Wu, J.S. Chen, C.F. Huang, C.C. Chen, K.C. Lu, P. Chu, H.K. Sytwu, Y.F. Lin, Approaching biomarkers of membranous nephropathy from a murine model to human disease, J. Biomed. Biotechnol. 2011 (2011) 581928.
[14] C.C. Wu, J.S. Chen, S.J. Chen, S.H. Lin, A. Chen, L.C. Chang, H.K. Sytwu, Y.F. Lin, Kinetics of adaptive immunity to cationic bovine serum albumin-induced membranous nephropathy, Kidney Int. 72 (2007) 831–840.
[15] C.C. Wu, J.S. Chen, S.H. Lin, A. Chen, H.K. Sytwu, Y.F. Lin, Experimental model of membranous nephropathy in mice: sequence of histological and biochemical events, Lab Anim. 42 (2008) 350–359.
[16] Y.S. Huang, C.C. Chang, T.C. Huang, Y.L. Hsieh, H.M. Shih, Daxx interacts with and modulates the activity of CREB, Cell Cycle 11 (2012) 99–108.
[17] T. Srivastava, M. Sharma, K.H. Yew, R. Sharma, R.S. Duncan, M.A. Saleem, E.T. McCarthy, A. Kats, P.A. Cudmore, U.S. Alon, C.J. Harrison, LPS and PAN-induced podocyte injury in an *in vitro* model of minimal change disease: changes in TLR profile, J. Cell Commun. Signal. 7 (2013) 49–60.
[18] A.M. Khalil, M. Guttman, M. Huarte, M. Garber, A. Raj, D. Rivea Morales, K. Thomas, A. Presser, B.E. Bernstein, A. van Oudenaarden, A. Regev, E.S. Lander, J.L. Rinn, Many human large intergenic noncoding RNAs associate with chromatin-modifying complexes and affect gene expression, Proc. Natl. Acad. Sci. U.S.A. 106 (2009) 11667–11672.
[19] J. Zhao, T.K. Ohsumi, J.T. Kung, Y. Ogawa, D.J. Grau, K. Sarma, J.J. Song, R.E. Kingston, M. Borowsky, J.T. Lee, Genome-wide identification of polycomb-associated RNAs by RIP-seq, Mol. Cell 40 (2010) 939–953.
[20] J.E. Froberg, L. Yang, J.T. Lee, Guided by RNAs: X-inactivation as a model for lncRNA function, J. Mol. Biol. 425 (2013) 3698–3706.
[21] D. Hessels, J.M. Klein Gunnewiek, I. van Oort, H.F. Karthaus, G.J. van Leenders, B. van Balken, L.A. Kiemeney, J.A. Witjes, J.A. Schalken, DD3(PCA3)-based molecular urine analysis for the diagnosis of prostate cancer, Eur. Urol. 44 (2003) 8–15. discussion 15–16.
[22] C.S. Bond, A.H. Fox, Paraspeckles: nuclear bodies built on long noncoding RNA, J. Cell Biol. 186 (2009) 637–644.
[23] J.T. Lee, Epigenetic regulation by long noncoding RNAs, Science 338 (2012) 1435–1439.
[24] R.A. Varier, H.T. Timmers, Histone lysine methylation and demethylation pathways in cancer, Biochim. Biophys. Acta 2011 (1815) 75–89.
[25] B. Li, M. Carey, J.L. Workman, The role of chromatin during transcription, Cell 128 (2007) 707–719.
[26] A.H. Fox, A.I. Lamond, Paraspeckles, Cold Spring Harbor Perspect. Biol. 2 (2010) a000687–a000700.
[27] J.T. Lee, M.S. Bartolomei, X-inactivation, imprinting, and long noncoding RNAs in health and disease, Cell 152 (2013) 1308–1323.
[28] T. Kumamoto, N. Tsukue, H. Takano, K. Takeda, S. Oshio, Fetal exposure to diesel exhaust affects X-chromosome inactivation factor expression in mice, J. Toxicol. Sci. 38 (2013) 245–254.
[29] K.C. Huang, P.H. Rao, C.C. Lau, E. Heard, S.K. Ng, C. Brown, S.C. Mok, R.S. Berkowitz, S.W. Ng, Relationship of *XIST* expression and responses of ovarian cancer to chemotherapy, Mol. Cancer Ther. 1 (2002) 769–776.
[30] M.A. Salvador, J. Wicinski, O. Cabaud, Y. Toiron, P. Finetti, E. Josselin, H. Lelievre, L. Kraus-Berthier, S. Depil, F. Bertucci, Y. Collette, D. Birnbaum, E. Charafe-Jauffret, C. Ginestier, The histone deacetylase inhibitor abexinostat induces cancer stem cells differentiation in breast cancer with low *xist* expression, Clin. Cancer Res. 19 (2013) 6520–6531.
[31] E.L. Greer, Y. Shi, Histone methylation: a dynamic mark in health, disease and inheritance, Nat. Rev. Genet. 13 (2012) 343–357.
[32] S. Rogenhofer, P. Kahl, S. Holzapfel, A. VON Ruecker, S.C. Mueller, J. Ellinger, Decreased levels of histone H3K9me1 indicate poor prognosis in patients with renal cell carcinoma, Anticancer Res. 32 (2012) 879–886.
[33] N. Brockdorff, A. Ashworth, G.F. Kay, V.M. McCabe, D.P. Norris, P.J. Cooper, S. Swift, S. Rastan, The product of the mouse *Xist* gene is a 15 kb inactive X-specific transcript containing no conserved ORF and located in the nucleus, Cell 71 (1992) 515–526.
[34] E. Yildirim, J.E. Kirby, D.E. Brown, F.E. Mercier, R.I. Sadreyev, D.T. Scadden, J.T. Lee, *Xist* RNA is a potent suppressor of hematologic cancer in mice, Cell 152 (2013) 727–742.